Therapeutics, Targets, and Chemical Biology

Transient Antiangiogenic Treatment Improves Delivery of Cytotoxic Compounds and Therapeutic Outcome in Lung Cancer

Sampurna Chatterjee[1,2,3], Caroline Wieczorek[1,2,3], Jakob Schöttle[1,2,3], Maike Siobal[1,2,3], Yvonne Hinze[4], Thomas Franz[4], Alexandra Florin[5], Joanna Adamczak[2], Lukas C. Heukamp[5], Bernd Neumaier[2], and Roland T. Ullrich[1,2,3]

Abstract

Extensive oncologic experience argues that the most efficacious applications of antiangiogenic agents rely upon a combination with cytotoxic drugs. Yet there remains a lack of clarity about how to optimize scheduling for such drug combinations. Prudent antiangiogenic therapy might transiently normalize blood vessels to improve tumor oxygenation and drug exposure. Using $[^{15}O]H_2O$ positron emission tomography imaging in a preclinical mouse model of non–small cell lung cancer, we observed that short-term treatment with the vascular endothelial growth factor receptor/platelet-derived growth factor receptor inhibitor PTK787 licensed a transient window of improved tumor blood flow. The improvement observed was associated with a reduced leakiness from tumor vessels, consistent with induction of a vascular normalization process. Initiation of a cytotoxic treatment in this window of tumor vessel normalization resulted in increased efficacy, as illustrated by improved outcomes of erlotinib administration after initial PTK787 treatment. Notably, intermittent PTK787 treatment also facilitated long-term tumor regression. In summary, our findings offer strong evidence that short-term antiangiogenic therapy can promote a transient vessel normalization process that improves the delivery and efficacy of a targeted cytotoxic drug. *Cancer Res; 74(10); 1–9. ©2014 AACR.*

Introduction

Solid tumors cannot grow without access to and recruitment of blood vessels (1, 2). Tumor vessels are characterized by a leaky, disorganized, and abnormal phenotype (3). This leakiness leads to extravasation of plasma proteins, resulting in a high interstitial fluid pressure within tumors that interferes with the delivery of drugs (4). Moreover, this abnormal phenotype of tumor vasculature supports tumor progression and resistance to treatment. The goal of antiangiogenic treatment is to inhibit tumor vessel growth, thus abrogating the delivery of nutrients and oxygen to the tumor. Antiangiogenic compounds target either angiogenic growth factors such as bevacizumab (anti-VEGF) or receptor kinases that are known to regulate tumor angiogenesis such as vascular endothelial growth factor receptor (VEGFR) and platelet-derived growth factor receptor (PDGFR). However, recent data indicate that a reduction in tumor vessels induced by antiangiogenic treatment using an antibody against VEGFR2 (DC101) results in an inhibition of tumor growth but on the other hand permits tumor invasiveness (5). This increase in invasiveness is most probably because of elevated hypoxia within the tumor during antiangiogenic therapy (6).

Nevertheless there is strong evidence that transient application of antiangiogenic agents can "normalize" the abnormal tumor microvessels (7, 8). This prudent application of antiangiogenic therapy might result in effective uptake of drugs and oxygen in the tumor-enhancing cytotoxic therapeutic outcome in cancer therapy (4, 9). Moreover, structurally and functionally abnormal blood vessels impair blood flow into the tumor contributing to an aggressive hypoxic microenvironment rendering the tumor unresponsive to traditional cytotoxic treatment regimes (10).

Using MRI we could recently demonstrate that short-term antiangiogenic treatment with a small molecule protein kinase inhibitor Vatalanib (PTK787) results in a reduction of vessel leakiness (11). Based on these findings we speculate that antiangiogenic treatment induced normalization of tumor vessels might increase tumor blood flow and reduce interstitial fluid pressure (IFP). This reduction of the IFP and increase of tumor blood flow during antiangiogenic treatment might improve anticancer drug delivery and, thus, treatment efficacy (12).

Authors' Affiliations: [1]Clinic I of Internal Medicine and Center for Integrated Oncology, University Hospital Cologne; [2]Max Planck Institute for Neurological Research; [3]Center for Molecular Medicine; [4]Max Planck Institute for Biology of Aging; and [5]Institute of Pathology, University Hospital Medical School, Cologne, Germany

Corresponding Author: Roland T. Ullrich, Max Planck Institute for Neurological Research with Klaus-Joachim-Zülch Laboratories of the Max-Planck-Society and the Medical Faculty of the University of Cologne, 50931 Cologne, Germany. Phone: 49-221-4726-306; Fax: 49-221-4726-298; E-mail: ullrich@nf.mpg.de

American Association for Cancer Research

PTK787 (ZK 222584) and ZD6474 are potent inhibitors of VEGFR tyrosine kinases, PDGFRβ tyrosine kinase and c-Kit whereas ZD6474 in addition targets the EGF receptor (EGFR) and RET (13, 14). We here sought to apply a multimodal imaging approach to monitor tumor blood flow *in vivo* to assess the normalization window during prudent antiangiogenic treatment using the tyrosine kinase inhibitors PTK787 and ZD6474. Imaging tumor vessel normalization induced by prudent antiangiogenic treatment was used to improve drug delivery of targeted compounds such as erlotinib and GDC0941.

Materials and Methods

Cell lines and reagents

Non–small cell lung cancer (NSCLC) cell line H1975 was purchased from the American Type Culture Collection. PC9 was purchased from European Collection of Cell Cultures. Both cell lines were maintained in RPMI-1640 medium enriched with 10% FCS and 1% penicillin + streptomycin. ZD6474, PTK787, and erlotinib were purchased from LC labs and GDC0941 from Axon Medchem. Compound stocks were stored at $-20°C$ and dissolved in dimethyl sulfoxide *in vitro*. For *in vivo* studies, erlotinib was dissolved in 6% Captisol (CyDex Inc.) at a concentration of 9 mg/mL. GDC0941 was dissolved in MCT (0.5% methylcellulose with 0.2% Tween-80 in distilled water) at concentrations of 22.5 mg/mL (monotherapy) and 15 mg/mL (in combination with antiangiogenic therapy). ZD6474 and PTK787 were dissolved in sterilized, deionized water with 1% Tween 80 at a concentration of 10 mg/mL. All solutions were stored on a rotating device at $4°C$ for animal therapy.

Western blotting

Western blotting was performed as described previously (15). For Western blotting, the following antibodies were used: β-actin (clone C4; MPBiomedicals LLC), pEGFR, pAKT (S473), pERK (Cell Signaling Technology), anti-rabbit-horseradish peroxidase (HRP) antibody, and anti-mouse-HRP antibody (Millipore).

Immunofluorescence

Vascular leakage was assessed by intravenous injection of 0.1 mL 10 mg/mL FITC-dextran (200,000 kDa) from Sigma. After 30 minutes, mice were anesthetized followed by perfusion with 4% paraformaldehyde injected into the aorta via an incision in the left ventricle and washed one time with PBS. Blood and fixative passaged out via the right atrium. Tumor sections were collected and immersed in 30% sucrose solution until samples dropped to the bottom of the vials. A cold bath was prepared with dry ice and methanol. Tissue Tek wells were labeled and filled up with Jung tissue freezing medium (Leica Biosystems). Excess sucrose was removed from tissues and placed in the center of wells and frozen by floating them on the methanol bath. Blocks were stored at $-20°C$ and sliced at 10 to 20 μm on cryostat. Slides were dried at room temperature for at least 2 hours and stained with anti-mouse CD31 (1:25; BD Pharmingen), anti-pVEGFR-2 (1:300; Cell Signaling Technology), fixed and processed for analysis in a Biorevo (Keyence) BZ-9000 microscope.

Tumor samples and immunohistochemistry

All tumors were collected after perfusion, stored in 4% paraformaldehyde overnight, and transferred to PBS. Tissues were embedded in paraffin following standard protocol and stained with primary antibodies as follows: mouse CD31 (1:25; BD Pharmingen), cleaved caspase-3 (1:750; Cell Signaling), pAKT (1:25; Cell Signaling), and α-smooth muscle actin α-SMA (1:50; Abcam) for marking pericytes. Corresponding secondary antibody detection kits for reduced background on murine tissue were used (Histofine Simple Stain Mouse MAX PO; medac) and stained on an automated stainer (LabVision Autostainer 480 S; Thermo Scientific).

Xenograft experiments

All animal procedures were approved by the local animal protection committee and the local authorities (Bezirksregierung Köln). Eight weeks old healthy *nu/nu* athymic male mice weighing 30 g in an average were purchased from Janvier. Tumors were generated by subcutaneous injection of PC9 and H1975 tumor cells (5×10^5 cells/tumor). Tumor-bearing mice were treated by oral gavage with the following set-ups: PTK787 ($n = 8$ mice with 3 tumors/mouse) or ZD6474 ($n = 8$ mice with 3 tumors/mouse) 75 mg/kg daily as monotherapy, erlotinib 30 mg/kg daily as monotherapy ($n = 8$ mice with 3 tumors/mouse), GDC0941 75 mg/kg daily as monotherapy ($n = 8$ mice with 3 tumors/mouse), vehicle ($n = 5$ mice with 3 tumors/mouse), erlotinib 30 mg/kg ($n = 14$ mice with 3 tumors/mouse), or GDC0941 50 mg/kg ($n = 8$ mice with 3 tumors/mouse) pretreated with PTK787 and continued as monotherapy during indicated timespan. The size of tumors ranged between 70 and 125 mm^3. Monotherapy and vehicle of each drug was used as control. Tumor volume was recorded accordingly.

[^{15}O]H$_2$O/[^{18}F]FLT positron emission tomography imaging

Animals bearing macroscopic tumors were investigated on day 0 followed by start of treatment with PTK787 75 mg/kg or ZD6474 75 mg/kg daily, day 4, day 8, and day 18 using a FOCUS microPET scanner (Siemens Microsystems, Inc; max. transaxial resolution 1.3 mm). In total, 25 animals underwent [^{15}O]H$_2$O and [^{18}F]FLT imaging, each animal carried 3 tumors. The PTK787-treated group contained 15 animals, the vehicle-treated group 10 mice. All animals underwent positron emission tomography (PET) imaging at 4 different time points. Initially 32 animals were included in the study, 7 of 32 mice died during PET imaging. We calculated percentage changes in tracer uptake with day 0 as baseline for each time point and tumor. [^{15}O]H$_2$O PET imaging was performed before [^{18}F]FLT PET. [^{18}F]FLT PET was measured 1 hour after [^{15}O]H$_2$O PET. [^{15}O]H$_2$O was injected dynamically via tail vein and PET images were acquired for 2 minutes after injection of 400 μCi/mouse. [^{18}F]FLT was administered intravenously (200 μCi/mouse). PET imaging was performed 60 minutes after injection (16). Data evaluation was performed using in-house VINCI software. Data evaluation was based on a region of interest (ROI) analysis. For data analysis we used the maximal and the mean voxel radioactivity of the defined ROI within the tumors. The

size of tumors ranged between 70 and 125 mm^3. The mediastinum was chosen as a reference for determination of uptake ratio, because we observed constant uptake for [^{18}F]FLT in this region. The heart was used as reference for calculation of the [^{15}O]H$_2$O. All data were decay corrected.

Mass spectrometry

For absolute quantification of erlotinib and OSI-420 in positive ESI MRM (multi reaction monitoring) mode, a Acquitiy UPLC/Xevo TQ (Waters) with MassLynx and absolute quantification TargetLynx (Waters) were used. An Acquity UPLC BEH C18 1.7 μm, 2.1 × 50 mm column was used at 25°C. Solvent A was 0.1% formic acid (Biosolve) and B acetonitrile (Biosolve). A linear gradient from 95% A to 5% in 4.10 min at a flow rate of 0.4 mL/min was used. The following MRM transitions were used for erlotinib m/z 394.03 (M+H$^+$)$^+$ to 277.95 (quantifier), m/z 394.03 to 303.95 (qualifier), m/z 394.03 to 335.94 (qualifier), for OSI-420 m/z 380.03 to 277.85 (quantifier), m/z 380.03 to 249.89 (qualifier), m/z 380.03 to 321.93 (qualifier). All compounds were fresh prepared during 2 months and dissolved in 0.1% formic acid (Biosolve) prepared with 0.22 μm MilliQ-Water. With erlotinib eluting at 2.94 minutes a standard calibration curve was calculated using following concentrations: 0.2, 0.5, 1, 5, 20, 50, 150, 300, 500, and 750 ng/mL (prepared individually from stock solutions 100 μg/mL). With OSI-420 eluting at 2.51 minutes a standard calibration curve was calculated using following concentrations: 0.1, 0.5, 1, 2, 4, 6, 8, and 10 ng/mL (prepared individually from stock solutions 100 μg/mL). Correlation coefficient: $r < 0.990$; response type: external standard, area; curve type linear; weighting 1/×. The peak integrations were corrected manually, if necessary. Quality control standards of each standard were used during sample analysis and showed between 0.5% and 40% deviation respectively. Blanks after the standards, quality control and sample batch proved to be sufficient. No carry over was detected.

Statistics

Fisher exact tests were performed using R version 2.7.1 (http://www.r-project.org). Data are presented as mean ± SD in all figures where error bars are shown. A level of significance of $P < 0.05$ was chosen (where mentioned).

Results

Short-term anti-VEGFR/PDGFR treatment induces a time window of improved blood flow into the tumor

We used the human lung cancer cell line PC9. PTK787 treatment improved tumor blood flow after 4 days of treatment by 12% (day 0: SD = 7.47, range = 22.42%; day 4: SD = 9.15, range = 35.04%), as determined by changes of maximal voxel activity in [^{15}O]H$_2$O PET ([^{15}O]H$_2$O; Fig. 1A, right and B). We could measure a steady and significant increase in tumor blood flow by 33.58% (day 8: SD = 5.52, range = 34.57%) until day 8 of treatment with PTK787 (P-value < 0.001) probably mediated by a transient normalization of vessels followed by a sharp decrease of 17.23% (day 18: SD = 12.63, range = 48.66%) till day 18. In contrast, blood flow decreased consistently from day 4 to day 8 by 20.42% (day 0: SD = 4.52, range = 9.39%; day 4: SD

= 4.67, range = 8.60%; day 8: SD = 5.58, range = 12.89%), and by 30.75% until day 18 (day 18: SD = 0.63, range = 10.53%) in the vehicle-treated tumors (Fig. 1A, left and B). Simultaneously, uptake of 3′-deoxy-3′-[^{18}F]-fluoro-ʟ-thymidine, [^{18}F]FLT), a marker of proliferation (17), was increased by 51.08% from day 0 to day 4 (day 4: SD = 26.81, range = 527.31%) and by 76% form day 0 to day 8 (day 8: SD = 44.99, range = 532.67%; Supplementary Fig. S1A–S1C), suggesting that the cells continued to progress through the cell cycle. In concordance with the [^{18}F]FLT PET data, treatment of H1975 and PC9 cells with 10 or 20 μmol/L PTK787 did not reduce tumor cell proliferation *in vitro* (Supplementary Fig. S1D and S1E).

To investigate if improvement in blood flow can be also achieved by using other antiangiogenic agents, we used ZD6474, a tyrosine kinase inhibitor, that targets VEGFR2 and EGFR with additional activity against VEGFR3, VEGFR1, PDGFRβ, and the RET tyrosine kinase. We treated H1975 xenografts with ZD6474, which are resistant to EGFR inhibition because of the presence of T790M gatekeeper mutation of EGFR (15). There was an increase in blood flow by 21.39% (day 0: SD = 0.91, range = 10.12%; day 4: SD = 9.23, range = 38.58%, day 8: SD = 5.82, range = 30.15%) from day 0 to day 8 of ZD6474 treatment followed by a drop of 20.95% from day 0 to day 18. Vehicle-treated tumors displayed a stable decrease in blood flow by 8.95% from day 0 to day 8 and by 14.78% on day 18 (SD = 4.32, range = 12.11%; Supplementary Fig. S2A and S2B). Proliferation remained unaffected as measured by an increase in [^{18}F]FLT uptake by 67.1% from day 0 to day 4 (day 4: SD = 3.17, range = 193.5%) and by 78.02% form day 0 to day 8 (day 8: SD = 20.49, range = 675.8%; Supplementary Fig. S3A and S3B).

These data indicate that prudent anti-VEGFR/PDGFR treatment produces a short-lived time window of about 7 days when tumor vessels are transiently normalized, which can be monitored by an increase in blood flow by up to 50% into the tumor.

Short-time antiangiogenic treatment reduces leakiness and improves pericyte coverage in tumor blood vessels in xenografts

To elucidate if the improved blood flow into the tumors was indeed because of vessel normalization, permeability of the blood vessels were examined by fluorescence microscopy after tumor-bearing animals were perfused with FITC-dextran. Blood vessels of vehicle-treated tumors were dilated with aberrant morphologic pattern and displayed extensive leakiness associated with massive extravasation of FITC-dextran (Fig. 2A, left and Supplementary Fig. S3C) and correlated with high expression of CD31 and p-VEGFR2 (Fig. 2A, left). However, in tumors that were treated with PTK787 for 4 days, blood vessels showed strikingly reduced leakiness with almost no extravasation of FITC-dextran (Fig. 2A, right and Supplementary Fig. S3C) supported by 8-fold reduction in signal intensity (Fig. 2B) accompanied by diminished CD31 and p-VEGFR2 expression. (Fig. 2A, right). Tumor vasculature was characterized by abnormal and discontinuous pericyte lining of vessels as indicated by arrows on day 0 (Fig. 2C). Antiangiogenic treatment for 4 days transiently improved pericyte coverage in contrast to vehicle-treated tumors, which still exhibited incoherent pericyte coverage (Fig. 2C and Supplementary Fig.
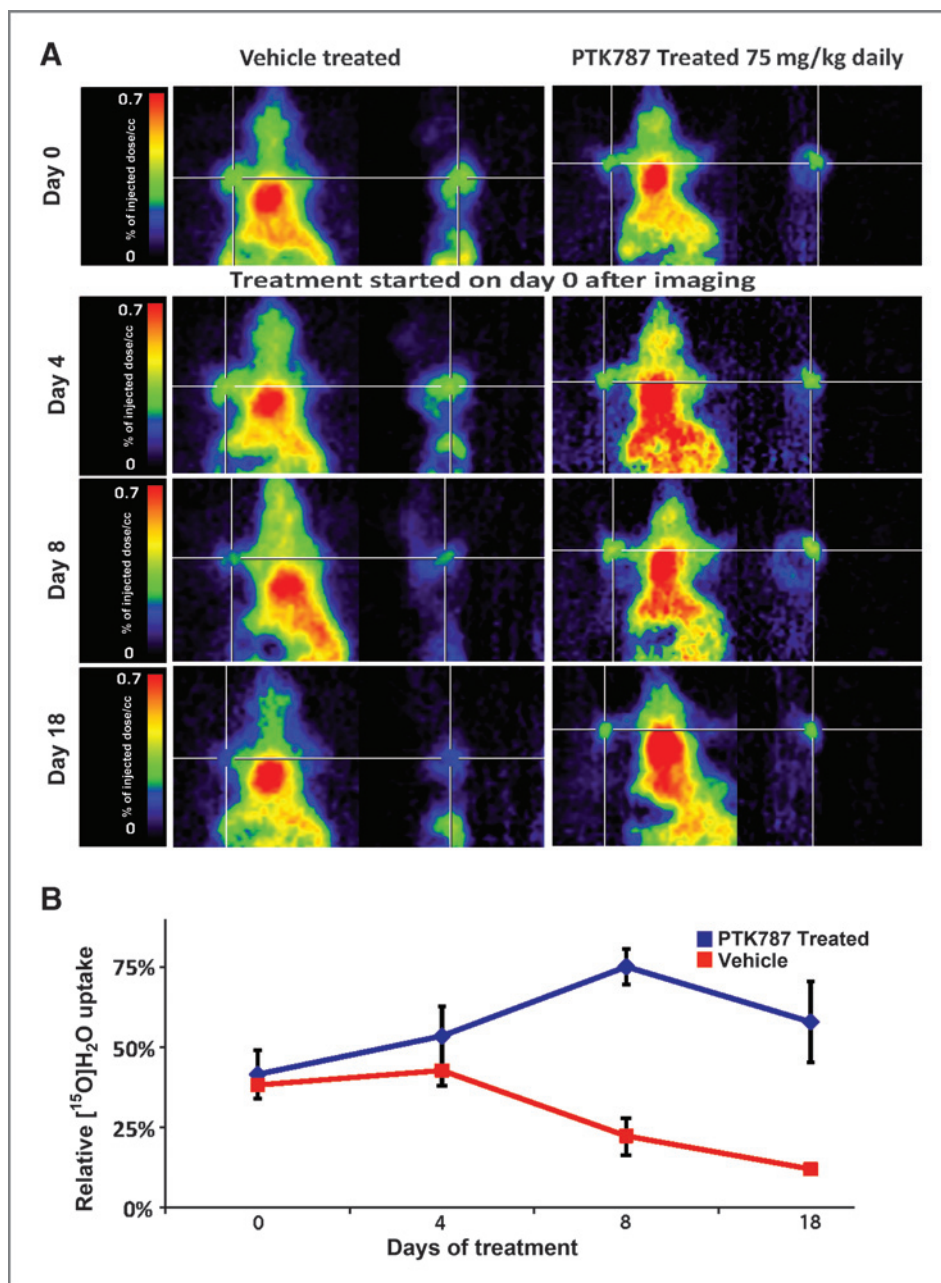
Figure 1. Multimodal imaging of tumor blood flow using [^{15}O]H$_2$O PET in xenografts (PC9). A, PET imaging was performed on nude mice with macroscopic subcutaneous tumors on day 0 (before start of therapy) and at the indicated time points after treatment with vehicle (left) and PTK787 (right). B, quantitative analysis of tumor blood perfusion before (day 0) and after 4, 8, and 18 days of PTK787 treatment (blue line) compared with vehicle sets (red line).
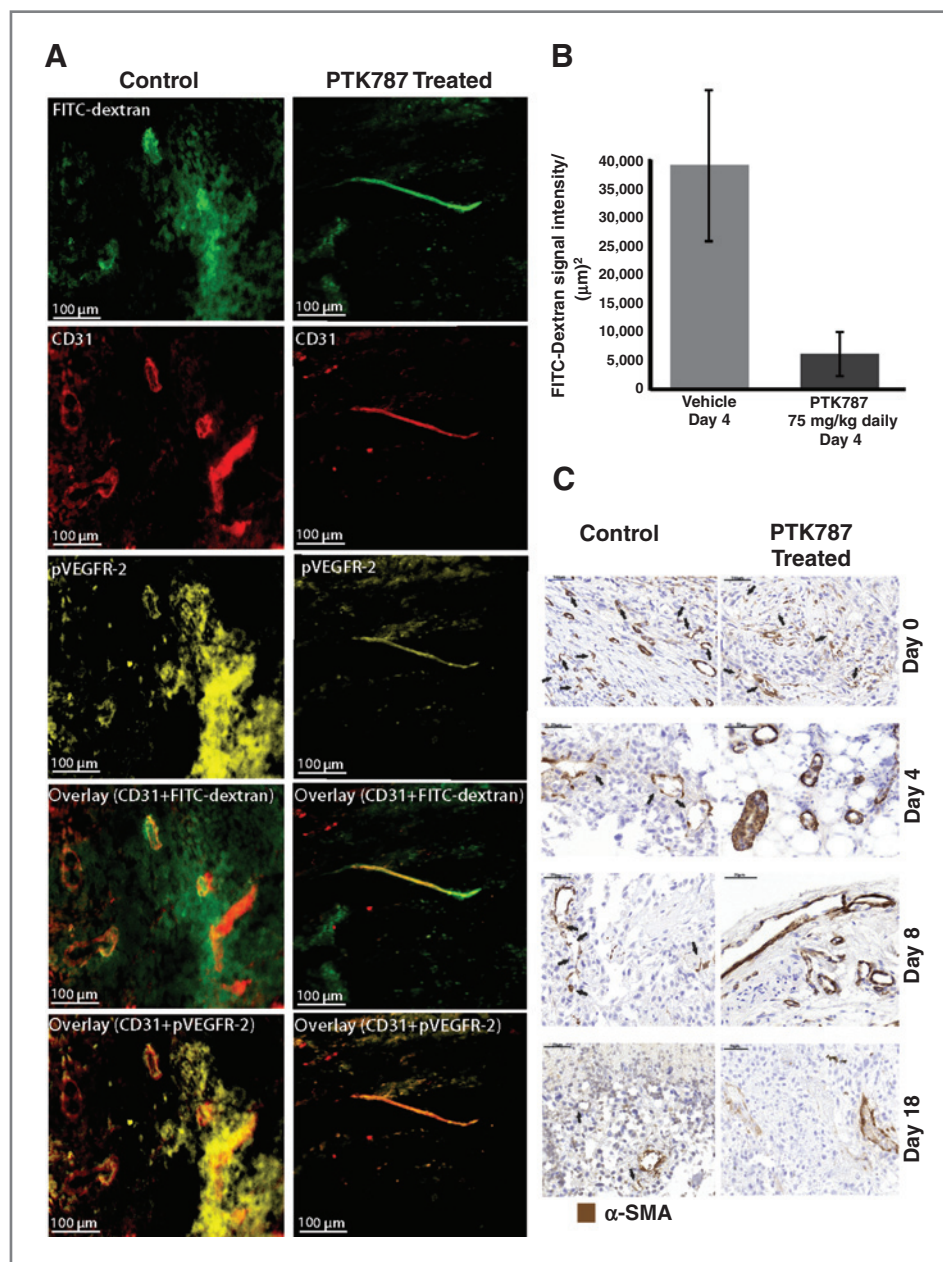
4A). PTK787 treatment also corrected the morphologic aberrations of the vessels with reduced tortuosity and improved maturity (Fig. 2C).

Pretreatment with antiangiogenic agents improves cytotoxic therapeutic outcome in NSCLC with enhanced delivery of erlotinib into the tumor

In the next step, we investigated if augmented blood flow induced by short-term antiangiogenic treatment had any improved therapeutic efficacy in NSCLC. Mice bearing macroscopic PC9 tumors were treated by an oral gavage of PTK787 (75 mg/kg daily) for 1 week. Because [^{15}O]H$_2$O PET data indicated that tumor blood flow improves within a

time window of 7 days of antiangiogenic therapy, erlotinib treatment was started within this "normalization window" from day 4 onward and continued as monotherapy for 13 days. Mice receiving erlotinib therapy pretreated with PTK787 had a sharp initial increase in tumor volume from 100% on day 1 to 221.28% (SD = 27.09, range = 162%) on day 4 followed by a massive reduction to 45.63% (SD = 7.11, range = 6.9%) on day 7, and finally almost complete shrinkage of tumor after 16 days of treatment (9.14% (SD = 3.2, range = 7.2%) of original mass left; Fig. 3A). Erlotinib as monotherapy restricted tumor proliferation, resulting in a slow reduction (up to 50% of tumor mass), but not as strong as with intermittent PTK787 treatment (P-value <

Figure 2. Blood vessel morphology and permeability. A, vascular leakage was assessed by intravenous injection of 0.1 mL 10 mg/mL FITC-dextran (200,000 kDa). Perfused tumors were collected and 10- to 20-μm-thick slices were stained with anti-mouseCD31 and anti-pVEGFR2 antibody, fixed and processed for microscopy control set (left) and PTK787-treated tumors (right). B, signal intensity of the total area of green staining (FITC-dextran) was quantified (4 fields per tumor in both control- and PTK787-treated groups). C, histology of tumors stained for α-SMA (brown, pericytes) comparing untreated vasculature (left) with PTK787 sets (right).

0.001; Fig. 3A). PTK787 monotherapy had similar effects like vehicle treatment (with an increase from 100% on day 1 to 245% and 220% (SD = 17.9, range = 38.8%) respectively on day 4; Fig. 3A).

To check if the normalized blood vessels were effectively delivering drugs into the tumors, we measured erlotinib concentration within the tumor via mass-spectrometric analysis. Under monotherapy with erlotinib, there was a slight improvement of the drug uptake into the tumor from day 1 (start of treatment) to day 4 by 20% (SD = 5.2, range = 34.16%; Fig. 3B). In contrast, tumors pretreated with PTK787 for 4 days displayed an increased erlotinib uptake by 140% (SD = 10.56, range = 35.64%) on the first day of erlotinib treatment (day 4), which improved up to 160% (SD = 11.04, range = 25.64%) on

day 8 (Fig. 3B). Monotherapy sets showed no further improvement in drug uptake, which was reduced by 42% (SD = 4.32, range = 23.72) on day 8 (Fig. 3B).

Western blot analysis of lysates from tumors treated with PTK787 and erlotinib showed an overtime decrease in pEGFR signal from day 1 to day 4 of treatment corresponding to pAKT and pERK levels (Fig. 3C). There was no change in signal intensity of pEGFR, pAKT, or pERK in the vehicle or monotherapy sets (PTK787 alone or erlotinib alone; Fig. 3C). Western blot analysis results correlated with histology where Ki67-positive cells were dramatically reduced in PTK787 pretreated tumors receiving erlotinib on day 1 compared with tumors receiving erlotinib as monotherapy on day 1 (Supplementary Fig. S4B). Ki67-positive cells were reduced further in number
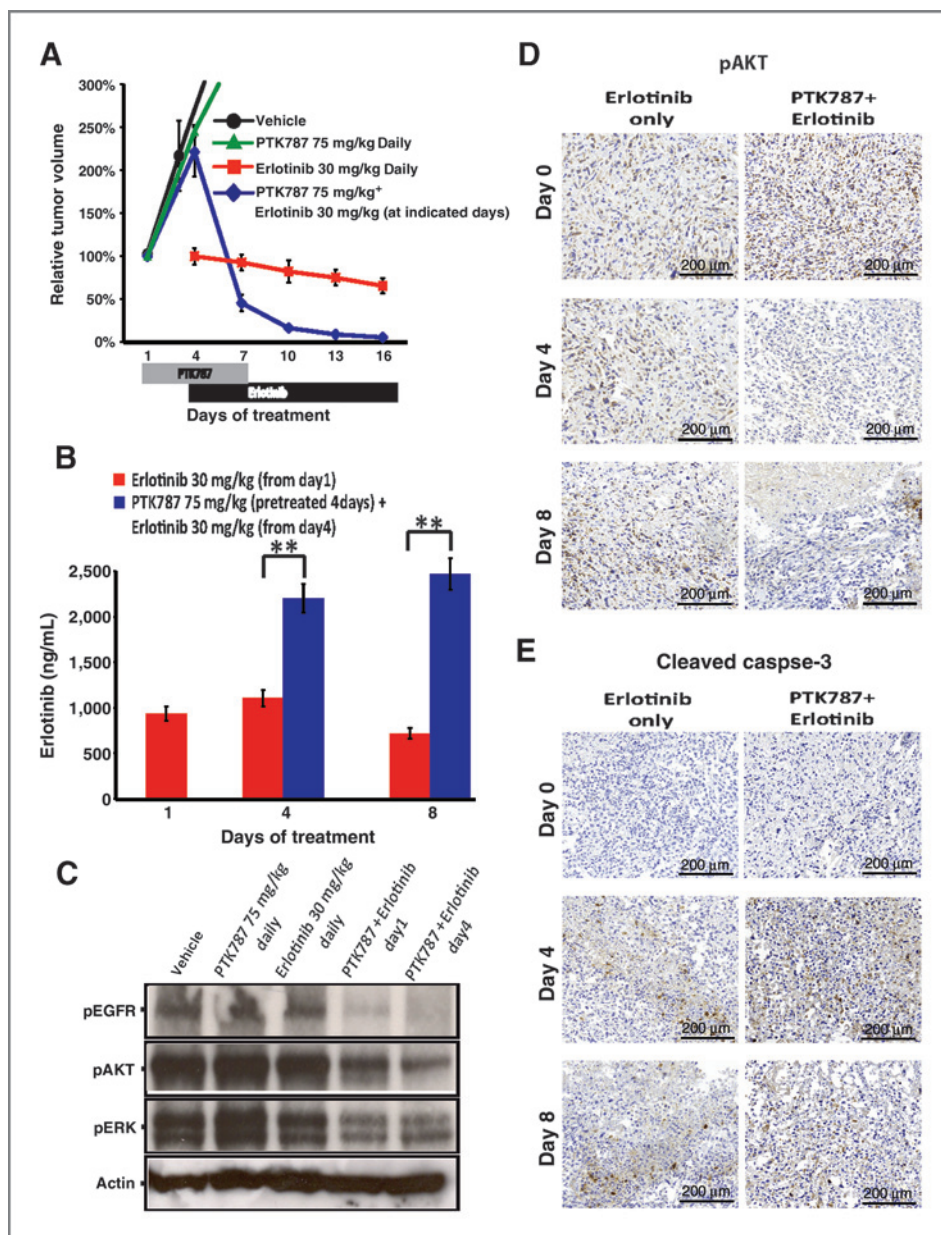
Figure 3. Prudent antiangiogenic treatment improves delivery of erlotinib into the tumor and promotes therapeutic outcome. A, tumor volumes in nude mice were recorded over time under treatment with PTK787 (75 mg/kg), erlotinib (30 mg/kg), and PTK787 (75 mg/kg) + erlotinib (30 mg/kg) and vehicle control at indicated days. B, quantification of erlotinib uptake as measured by mass spectrometry in PTK787 pretreated tumors (blue column) between day 4 and 8 compared with uptake in the tumors receiving erlotinib just as monotherapy (four independent tumors from different mice per set-up). C, tumor lysates were prepared from different therapy modules (as indicated) and immunoblotted with phospho-specific antibodies. Representative Western blots are shown. D, histology of tumor samples from C comparing pAKT expression between erlotinib monotherapy and erlotinib pretreated with PTK787 tumors on day 0 (before start of treatment) and on indicated days after therapy. E, induction of apoptosis (cleaved caspase-3) in erlotinib monotherapy and erlotinib pretreated with PTK787 tumors on day 0 (before start of treatment) and on indicated days after therapy.

from day 0 to day 4 until only a few Ki67-positive cells were left on day 8 in the tumors receiving erlotinib pretreated with PTK787 (Supplementary Fig. S4B). Histology results also showed complete inhibition of pAKT from day 0 to day 4 in PTK787 pretreated tumors receiving erlotinib (Fig. 3D). pAKT levels remain inhibited on day 8 with induction of necrosis (Fig. 3D). Even though tumor cells were healthy in both sets on day 0 (Fig. 3E), heavy induction of apoptosis (cleaved caspase-3) was detected in tumors receiving erlotinib pretreated with PTK787 on day 4 (Fig. 3E, right), which remained consistent on day 8 (Fig. 3E, right). However, in erlotinib monotherapy sets, there was only moderate induction of apoptosis overtime (Fig. 3E, left).
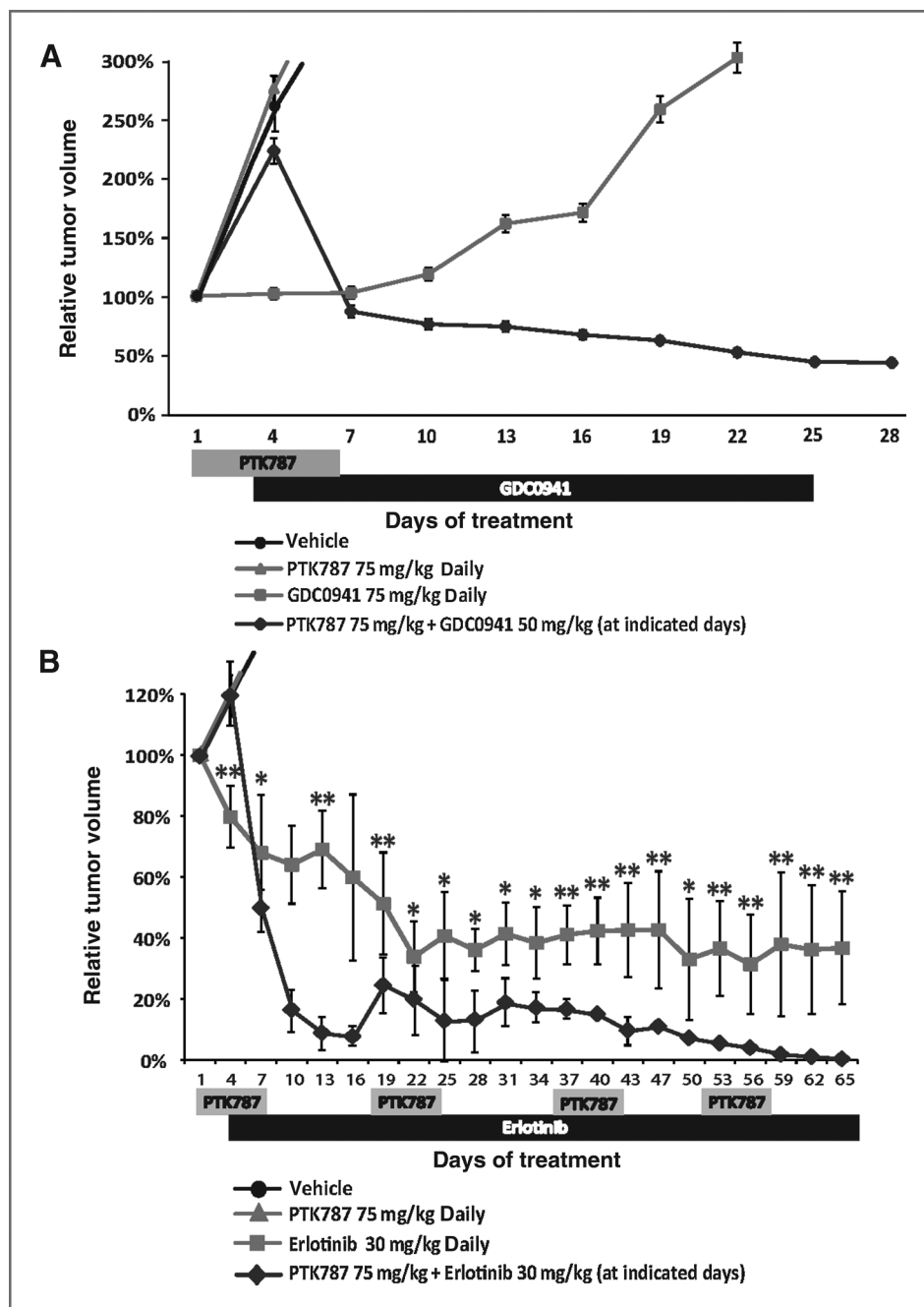
To confirm that this effect of tumor shrinkage was only because of better drug delivery facilitated by prudent anti-angiogenic treatment, macroscopic H1975 tumor bearing mice pretreated with PTK787 were treated with phosphoinositide 3-kinase inhibitor GDC0941. Tumors receiving GDC0941 therapy pretreated with PTK787 receded by 50% (SD = 4.7, range = 10.07) more than 28 days compared with just a mild growth inhibition observed in GDC0941 monotherapy sets, which tumor volumes surpassed by 250% (SD = 10.41, range = 22,10) on day 22 (Fig. 4A).

Intermittent antiangiogenic treatment facilitates long-term tumor regression

A long-term xenograft study with subcutaneous PC9 tumors was performed where mice were treated with a continuous dose of erlotinib combined with a short PTK787 treatment every 10 days. Tumors remained regressed in this combination

Figure 4. Short antiangiogenic treatment improves therapeutic outcome of GDC0941; long-term tumor regression with intermittent antiangiogenic therapy. PC9 cells were engrafted subcutaneously in nude mice and tumor volumes were recorded over time for either 28 days under treatment with PTK787 (75 mg/kg), GDC0941 (75 mg/kg) and PTK787 (75 mg/kg) + GDC0941 (50 mg/kg) at indicated days ($n = 6$ mice with 3 tumors/mouse for each set-up; A) or for 65 days under treatment with PTK787 (75 mg/kg), erlotinib (30 mg/kg), and erlotinib (30 mg/kg) with intermittent PTK787 treatment from day 1 to day 7, day 17 to day 25, day 35 to day 43 and day 51 to day 58 ($n = 6$ mice with 3 tumors/mouse for each set-up; B).

model over the entire time span of 65 days (Fig. 4B). However, in mice treated with erlotinib only, there was an initial tumor regression up to 40% of original tumor volume until day 22 followed by a stable disease (Fig. 4B).

Discussion

Using *in vivo* PET imaging we demonstrate that transient antiangiogenic treatment using PTK787 improves tumor blood flow *in vivo*. This transient tumor vessel normalization results in an improved delivery of targeted compounds such as

erlotinib into the tumor. Most strikingly, enhanced availability and distribution of erlotinib within the tumor induced by transient PTK787 treatment was followed by a significant increase in tumor shrinkage. This improvement in tumor response is consistent with recent findings demonstrating that high-dose EGFR-targeted drug exposure results in more efficient target inhibition (18).

Several mechanisms have been described as potential targets to improve the function of tumor vessels. Recently, Chakroborty and colleagues described Dopamine as a potential drug to improve the function of tumor vessels. The

normalization effect was mainly mediated by an upregulation of angiopoetin-1 and the Krüppel-like factor 2 (19). Similarly, treatment with the Cox-2 inhibitor apricoxib increased the maturity of tumor vessel in vivo (20). In line with our findings this vascular normalization effect was associated with a significantly enhanced efficacy of gemcitabine plus erlotinib (21). Tumor vessel normalization upon apricoxib treatment was primarily induced by a transient reduction in VEGF secretion within the tumor in vivo. Of note, the tumor vessel normalization effect was time and dose dependent (20). Rakesh Jain recently reported that the tumor vessel normalization effect induced by inhibition of the VEGF-VEGFR2 axis is time and dose dependent (22, 23). We applied $[^{15}O]H_2O$ PET imaging to decipher this time-dependent tumor vessel normalization effect. In line with the tumor vessel normalization hypothesis, tumor blood flow increased within the first 8 days of PTK787 treatment but again declined till day 18 of treatment accompanied by a decrease in pericyte coverage (19, 24). Thus, our data strongly indicate that tumor vessel normalization induced by PTK787 is time dependent. We found similar results with ZD6474, a tyrosine kinase inhibitor that primarily targets EGFR and VEGFR2 (13). As we applied H1975 xenografts that are resistant to EGFR treatment, the ZD6474 induced effect on the tumor vasculature seems to be mainly driven by inhibition of VEGFR2. Similarly, Huang and colleagues found that low-dose treatment with an anti-VEGFR2-antibody (DC101) results in an increase in pericyte coverage in a breast cancer in vivo model (25). These and our data indicate that the primary target to induce tumor vessel normalization is most probably VEGFR2. However, further investigations are required to decipher in detail the responsible tyrosine kinases that drive tumor vessel normalization.

In our study the implication of $[^{15}O]H_2O$-PET–guided use of PTK787 and ZD6474 treatment significantly improved the delivery of the cytotoxic compounds erlotinib and GDC0941. $[^{15}O]H_2O$ PET has been already successfully applied in patients with human lung cancer (26). Thus, $[^{15}O]H_2O$ PET reflects a highly accurate method that can easily be translated into clinical application. The implementation of $[^{15}O]H_2O$ PET enables to establish combined antiangiogenic and cytotoxic PET-guided treatment protocols in individual patients to improve the delivery of cytotoxic compounds.

Cytotoxic agents combined with antiangiogenic therapy has shown only little efficacy in patients with advanced stage NSCLC. In a recent phase III trial, the addition of bevacizumab to chemotherapy for newly diagnosed glioblastoma did not improve overall survival (27). In a recent human study, docetaxel uptake was reduced in NSCLC after patients were administered with bevacizumab (28). These data indicate that inhibition of VEGF potentially bears an antivascular than tumor vessel normalization effect supporting the notion that scheduling and dosing of the antiangiogenic treatment is essential to induce and maintain tumor vessel normalization. This is also confirmed by our PET data as the vascular normalization effect seems to be transient as continuous treatment with PTK787 or ZD6474 result in a reduction in tumor flow after more than 8 days of treatment. Our data strengthen the use of $[^{15}O]H_2O$ PET in clinical studies to define the optimal dose and schedule of antiangiogenic drugs such as bevacizumab and PTK787 to improve the delivery of cytotoxic drugs in to the tumor.

In summary, our findings are consistent with the vascular normalization hypothesis and are indicative of the fact that prudent antiangiogenic therapy leads to evanescent vessel normalization, resulting in better cytotoxic therapeutic outcome. However, optimal designs of drug scheduling and efficient imaging techniques are absolutely indispensable to achieve maximal clinical outcome.

Disclosure of Potential Conflicts of Interest

No potential conflicts of interest were disclosed.

Authors' Contributions

Conception and design: S. Chatterjee, B. Neumaier, R.T. Ullrich
Development of methodology: S. Chatterjee, B. Neumaier, R.T. Ullrich
Acquisition of data (provided animals, acquired and managed patients, provided facilities, etc.): S. Chatterjee, C. Wieczorek, J. Schöttle, M. Siobal, Y. Hinze, T. Franz, A. Florin, L.C. Heukamp, R.T. Ullrich
Analysis and interpretation of data (e.g., statistical analysis, biostatistics, computational analysis): S. Chatterjee, J. Schöttle, L.C. Heukamp, R.T. Ullrich
Writing, review, and or revision of the manuscript: S. Chatterjee, T. Franz, B. Neumaier, R.T. Ullrich
Administrative, technical, or material support (i.e., reporting or organizing data, constructing databases): S. Chatterjee, M. Siobal, A. Florin, J. Adamczak, L.C. Heukamp, B. Neumaier, R.T. Ullrich
Study supervision: R.T. Ullrich

References

1. Folkman J. Tumor angiogenesis: therapeutic implications. N Engl J Med 1971;285:1182–6.
2. Rak J, Yu JL, Kerbel RS, Coomber BL. What do oncogenic mutations have to do with angiogenesis/vascular dependence of tumors? Cancer Res 2002;62:1931–4.
3. Mazzone M, Dettori D, Leite de Oliveira R, Loges S, Schmidt T, Jonckx B, et al. Heterozygous deficiency of PHD2 restores tumor oxygenation and inhibits metastasis via endothelial normalization. Cell 2009;136: 839–51.
4. Jain RK. Normalization of tumor vasculature: an emerging concept in antiangiogenic therapy. Science (New York, NY). 2005;307:58–62.
5. Paez-Ribes M, Allen E, Hudock J, Takeda T, Okuyama H, Vinals F, et al. Antiangiogenic therapy elicits malignant progression of tumors to increased local invasion and distant metastasis. Cancer Cell 2009; 15:220–31.
6. Rapisarda A, Melillo G. Role of the hypoxic tumor microenvironment in the resistance to anti-angiogenic therapies. Drug Resist Updat 2009; 12:74–80.

7. Jain RK. Normalizing tumor vasculature with anti-angiogenic therapy: a new paradigm for combination therapy. Nat Med 2001;7:987–9.

8. Zhang Q, Bindokas V, Shen J, Fan H, Hoffman RM, Xing HR. Time-course imaging of therapeutic functional tumor vascular normalization by antiangiogenic agents. Mol Cancer Ther 2011;10:1173–84.

9. Winkler F, Kozin SV, Tong RT, Chae SS, Booth MF, Garkavtsev I, et al. Kinetics of vascular normalization by VEGFR2 blockade governs brain tumor response to radiation: role of oxygenation, angiopoietin-1, and matrix metalloproteinases. Cancer Cell 2004;6:553–63.

10. Fukumura D, Duda DG, Munn LL, Jain RK. Tumor microvasculature and microenvironment: novel insights through intravital imaging in pre-clinical models. Microcirculation 2010;17:206–25.

11. Ullrich RT, Jikeli JF, Diedenhofen M, Bohm-Sturm P, Unruh M, Vollmar S, et al. In vivo visualization of tumor microvessel density and response to anti-angiogenic treatment by high resolution MRI in mice. PLoS ONE 2011;6:e19592.

12. Kerbel RS. Antiangiogenic therapy: a universal chemosensitization strategy for cancer? Science (New York, NY) 2006;312:1171–5.

13. Wedge SR, Ogilvie DJ, Dukes M, Kendrew J, Chester R, Jackson JA, et al. ZD6474 inhibits vascular endothelial growth factor signaling, angiogenesis, and tumor growth following oral administration. Cancer Res 2002;62:4645–55.

14. Wood JM, Bold G, Buchdunger E, Cozens R, Ferrari S, Frei J, et al. PTK787/ZK 222584, a novel and potent inhibitor of vascular endothelial growth factor receptor tyrosine kinases, impairs vascular endothelial growth factor-induced responses and tumor growth after oral administration. Cancer Res 2000;60:2178–89.

15. Chatterjee S, Heukamp LC, Siobal M, Schottle J, Wieczorek C, Peifer M, et al. Tumor VEGF:VEGFR2 autocrine feed-forward loop triggers angiogenesis in lung cancer. J Clin Invest 2013;123:3183.

16. Ullrich RT, Zander T, Neumaier B, Koker M, Shimamura T, Waerzeggers Y, et al. Early detection of erlotinib treatment response in NSCLC by 3′-deoxy-3′-[F]-fluoro-L-thymidine ([F]FLT) positron emission tomography (PET). PLoS ONE 2008;3:e3908.

17. Shields AF, Grierson JR, Dohmen BM, Machulla HJ, Stayanoff JC, Lawhorn-Crews JM, et al. Imaging proliferation in vivo with [F-18]FLT and positron emission tomography. Nat Med 1998;4:1334–6.

18. Shah NP, Kasap C, Weier C, Balbas M, Nicoll JM, Bleickardt E, et al. Transient potent BCR-ABL inhibition is sufficient to commit chronic myeloid leukemia cells irreversibly to apoptosis. Cancer Cell 2008; 14:485–93.

19. Chakroborty D, Sarkar C, Yu H, Wang J, Liu Z, Dasgupta PS, et al. Dopamine stabilizes tumor blood vessels by up-regulating angiopoietin 1 expression in pericytes and Kruppel-like factor-2 expression in tumor endothelial cells. Proc Natl Acad Sci U S A 2011;108:20730–5.

20. Kirane A, Toombs JE, Larsen JE, Ostapoff KT, Meshaw KR, Zaknoen S, et al. Epithelial-mesenchymal transition increases tumor sensitivity to COX-2 inhibition by apricoxib. Carcinogenesis 2012; 33:1639–46.

21. Kirane A, Toombs JE, Ostapoff K, Carbon JG, Zaknoen S, Braunfeld J, et al. Apricoxib, a novel inhibitor of COX-2, markedly improves standard therapy response in molecularly defined models of pancreatic cancer. Clin Cancer Res 2012;18:5031–42.

22. Jain RK. Normalizing tumor microenvironment to treat cancer: bench to bedside to biomarkers. J Clin Oncol 2013;31:2205–18.

23. Huang Y, Stylianopoulos T, Duda DG, Fukumura D, Jain RK. Benefits of vascular normalization are dose and time dependent–letter. Cancer Res 2013;73:7144–6.

24. Jain RK, Booth MF. What brings pericytes to tumor vessels? J Clin Invest 2003;112:1134–6.

25. Huang Y, Yuan J, Righi E, Kamoun WS, Ancukiewicz M, Nezivar J, et al. Vascular normalizing doses of antiangiogenic treatment reprogram the immunosuppressive tumor microenvironment and enhance immunotherapy. Proc Natl Acad Sci U S A 2012;109:17561–6.

26. de Langen AJ, van den Boogaart V, Lubberink M, Backes WH, Marcus JT, van Tinteren H, et al. Monitoring response to antiangiogenic therapy in non-small cell lung cancer using imaging markers derived from PET and dynamic contrast-enhanced MRI. J Nucl Med 2011; 52:48–55.

27. Gilbert MR, Dignam J, Won M, Blumenthal DT, Vogelbaum MA, Aldape KD, et al. Phase III double-blind placebo-controlled trial evaluating bevacizumab (Bev) in patients (Pts) with newly diagnosed glioblastoma (GBM). J Clin Oncol 31, 2013 (suppl; abstr 1). 2013;2013 ASCO Annual Meeting.

28. Van der Veldt AA, Lubberink M, Bahce I, Walraven M, de Boer MP, Greuter HN, et al. Rapid decrease in delivery of chemotherapy to tumors after anti-VEGF therapy: implications for scheduling of anti-angiogenic drugs. Cancer Cell 2012;21:82–91.

Cancer Research

The Journal of Cancer Research (1916–1930) | The American Journal of Cancer (1931–1940)

AACR American Association for Cancer Research

Transient Antiangiogenic Treatment Improves Delivery of Cytotoxic Compounds and Therapeutic Outcome in Lung Cancer

Sampurna Chatterjee, Caroline Wieczorek, Jakob Schöttle, et al.

Updated version	Access the most recent version of this article at: doi:10.1158/0008-5472.CAN-13-2986
Supplementary Material	Access the most recent supplemental material at: http://cancerres.aacrjournals.org/content/suppl/2014/03/27/0008-5472.CAN-13-2986.DC1.html

E-mail alerts	Sign up to receive free email-alerts related to this article or journal.
Reprints and Subscriptions	To order reprints of this article or to subscribe to the journal, contact the AACR Publications Department at pubs@aacr.org.
Permissions	To request permission to re-use all or part of this article, contact the AACR Publications Department at permissions@aacr.org.